Field-Dependent Electron Mobility in Silicon Between 8 and 77 K—A Semi-empirical Model

HÉCTOR DE LOS SANTOS AND JEFFERY L. GRAY, MEMBER, IEEE

Abstract—**The development of a semi-empirical model that predicts the electron mobility in silicon as a function of the electric field in the ⟨100⟩ direction, the doping density, and the temperature for the temperature range 8 to 77 K is discussed. The approach integrates the empirical formulas relating drift velocity and mobility to electric field, developed by Caughey and Thomas, the experimental data obtained by Canali *et al.*, for hyperpure silicon at low temperatures, the theory of scattering rate scaling proposed by Thornber, and the simulation of electron transport via the Monte Carlo method. Figures showing the resulting electron drift velocity under various conditions of doping and temperature are included.**

I. INTRODUCTION

THE numerical modeling of infrared (IR) detectors is, in principle, no different than that of other semiconductor devices such as solar cells, bipolar transistors, MOSFET's, diodes, etc. All of these devices can be characterized by a set of physical parameters such as mobility and lifetime, as well as technological parameters including geometry, impurity profile, and so on [1]. One aspect that distinguishes the modeling of IR detectors from that of other semiconductor devices, however, is the range of temperatures for which the model is expected to be accurate. While, for the most part, the modeling of BJT's, MOSFET's, diodes, etc., is geared toward reproducing and predicting device behavior near room temperature, i.e., 300 K, that of IR detectors is geared toward reproducing and predicting phenomena at much lower temperatures.

The numerical modeling of extrinsic photoconductor detectors, for instance, requires that models for the electron mobility be known at temperatures near that of liquid helium, i.e., close to 4.2 K. Empirical expressions that fit the variation of the electron mobility as a function of electric field, temperature, and doping density have been deduced from an analysis of published experimental data [2], [3]. Most of these data, however, have been obtained at temperatures much higher than the present range of interest. As a result, the empirical fits that are a consequence of the said experimental data are lacking in our present situation. The problem at hand then is that of generating the desired data at low temperature via theoretical calculations.

This paper presents a procedure to be followed in estimating the electron mobility in silicon at low temperatures, including its electric field and doping density dependences. In Section II the approach followed in obtaining the characteristics is described, and in Section III the results are presented.

II. MODELING ELECTRON MOBILITY AT LOW TEMPERATURES IN SILICON

A. Electric Field Dependence

The point of departure consists of the drift velocity versus electric field characteristics for hyperpure silicon in the ⟨100⟩ direction as experimentally determined by Canali *et al.* [4] for a range of temperatures and is shown in Fig. 1. For electric fields below 100 V/cm, the characteristics show negative differential mobility (NDM) effects. These effects are said to be due to a change in the repopulation of the valleys at the minimum of the conduction band, from that pertaining to a field applied along ⟨111⟩ to that pertaining to a field applied along ⟨100⟩, as the field increases [4]. Since the NDM effects occur at such low electric fields and for so short a range of fields, it is expected that its neglect will have insignificant consequences when devices that operate at fields above 100 V/cm are considered. Accordingly, this work will not try to predict the NDM features but will focus on predicting the electric field dependence for fields above 100 V/cm. The field variation of these curves for electric fields greater than 100 V/cm is approximated in an excellent fashion by the empirical expression proposed by Caughey and Thomas [2], namely

$$v = \frac{\mu_0 E}{\left[1 + \left(\mu_0 \frac{E}{v_s}\right)^{\beta}\right]^{1/\beta}} \tag{1}$$

Manuscript received April 19, 1988; revised August 1, 1988. This work was supported under a grant from the Hughes Aircraft Company. H. De Los Santos is a Patricia Roberts Harris Fellow.

The authors are with the School of Electrical Engineering, Purdue University, West Lafayette, IN 47907.

IEEE Log Number 8823675.

0018-9383/88/1100-1972$01.00 © 1988 IEEE

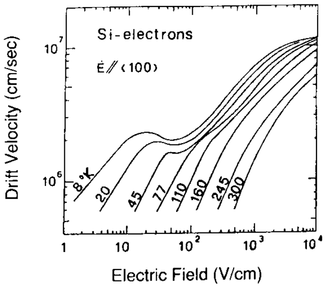

Fig. 1. Experimental electron drift velocity as a function of electric field applied parallel to a ⟨100⟩ direction at various temperatures. After Canali *et al.* [4].

where μ_0 and v_s are interpreted as the apparent low-field mobility and saturation velocity, respectively, and E is the electric field. The cord mobility (ratio of velocity to field strength) is given by

$$\mu = \frac{\mu_0}{\left[1 + \left(\mu_0 \dfrac{E}{v_s}\right)^{\beta}\right]^{1/\beta}}. \tag{2}$$

This model is further generalized to include temperature and doping dependences.

B. Temperature and Doping Dependence

In order to model the temperature dependence, a fit of (1) was made to each of the pertinent curves in Fig. 1. From these fits the variations in the parameters μ_0, v_s, and β with temperature were found to be approximated, to within a maximum error of 14 percent, as follows:

$$\mu_0(T) = 2.69 \times 10^4 \cdot T^{0.02}\ (\text{cm}^2/\text{V} \cdot \text{s}) \tag{3}$$

$$v_s(T) = 9.83 \times 10^6 \cdot T^{0.18}\ (\text{cm/s}) \tag{4}$$

$$\beta(T) = 1.23 \cdot T^{-0.24}. \tag{5}$$

The lack of doping-dependent drift velocity versus electric field data at low temperatures has prompted their theoretical determination.

The approach used to obtain the doping dependence is based on the theory of scattering rate scaling proposed by Thornber [5], [6]. According to this theory, if, in the absence of a magnetic field, the carrier distribution function changes as a result of a uniform scaling in the magnitude and momentum of the scattering rates, the respective drift velocity versus electric field relations before scaling ($v(E)$) and after scaling ($v_{\Gamma,\gamma}(E)$) are related as follows:

$$v_{\Gamma,\gamma}(E) = \gamma \cdot v(E/\gamma\Gamma) \tag{6}$$

where Γ and γ are the magnitude and momentum scaling factors of the scattering rates, respectively. In terms of the drift velocity model adopted here, this result takes the form

$$v_{\Gamma,\gamma}(E) = \frac{\mu_0 E/\Gamma}{\left[1 + \left(\mu_0 \dfrac{E}{v_s \gamma \Gamma}\right)^{\beta}\right]^{1/\beta}} \tag{7}$$

where μ_0, v_s, and β are the parameters that fit the drift velocity versus electric field characteristic at the temperature of interest. Knowing the drift velocity versus electric field characteristics for the temperature of interest then allows for the relation corresponding to any other doping(s) to be immediately determined, once Γ and γ are known for that temperature.

In order to obtain Γ and γ, (7) has been fitted to the high-field drift velocity versus electric field characteristics for a number of doping densities and temperatures of interest. These characteristics have been obtained via Monte Carlo simulations of the transport of electrons in the ⟨100⟩ direction, including nonparabolicity, using the methodology given in [7]. The scattering mechanisms that are most effective at the temperatures of interest have been identified by Pearson and Bardeen [8] to be neutral and ionized impurity scattering, and lattice scattering. The model used to represent the ionized impurity scattering mechanism was that of Conwell and Weisskopf [9]. Following Canali *et al.* [4], [7], neutral impurity scattering was not included. Two lattice scattering mechanisms were included, namely, intravalley inelastic acoustic phonon scattering and equivalent intervalley phonon scattering. The models used for these were those of Conwell [10] and Fawcett *et al.* [11], respectively. Selection rules forbid intravalley optical-phonon interactions for electrons along the ⟨100⟩ directions [7], and hence, this scattering mechanism was not included. Even though selection rules also "forbid" the low-energy intervalley phonons, their previous use has resulted in an improved agreement with experiments [4]. Therefore, they were included in the three f and the three g equivalent intervalley scatterings. All these scattering mechanisms are discussed in detail in [7].

Since, as seen from (7), the drift velocity is highly sensitive to errors in the scaling factors, it was deemed preferable to use a table look-up scheme in incorporating their values into (7). The actual values obtained for Γ and $\gamma\Gamma$ are given in Table I.

III. Results

To evaluate our approach we have attempted to reproduce the experimental results of Fig. 1 for temperatures between 8 and 77 K and fields above 100 V/cm. The results are shown in Fig. 2. As can be seen, our predicted characteristics agree reasonably well with the experimental ones. The discrepancy is mainly due to the fact that at the lowest energies the rates of the main scattering mechanisms, ionized impurity and equivalent intervalley

TABLE I
SCATTERING RATE SCALING FACTORS

	T = 8K										
Nd(cm^{-3})	$3\cdot10^{12}$	10^{14}	$5\cdot10^{14}$	10^{15}	$5\cdot10^{15}$	$7\cdot10^{15}$	10^{16}	$5\cdot10^{16}$	10^{17}	$5\cdot10^{17}$	10^{18}
Γ	2.14	3.46	5.58	7.38	24.00	32.02	35.75	70.64	116.07	350.78	481.44
$\gamma\Gamma$	1.87	3.54	6.40	9.56	133.00	$1.23\cdot10^{3}$	$1.12\cdot10^{7}$	$2.47\cdot10^{6}$	$4.64\cdot10^{6}$	$8.12\cdot10^{6}$	$1.34\cdot10^{5}$
	T = 10K										
Nd(cm^{-3})	$3\cdot10^{12}$	10^{14}	$5\cdot10^{14}$	10^{15}	$5\cdot10^{15}$	$7\cdot10^{15}$	10^{16}	$5\cdot10^{16}$	10^{17}	$5\cdot10^{17}$	10^{18}
Γ	1.63	2.76	5.03	6.76	23.26	34.14	37.00	77.23	121.37	314.62	458.22
$\gamma\Gamma$	1.33	2.55	5.63	8.08	123.5	$3.31\cdot10^{5}$	$8.33\cdot10^{6}$	$1.20\cdot10^{7}$	$4.53\cdot10^{6}$	$6.69\cdot10^{6}$	$1.77\cdot10^{7}$
	T = 12K										
Nd(cm^{-3})	$3\cdot10^{12}$	10^{14}	$5\cdot10^{14}$	10^{15}	$5\cdot10^{15}$	$7\cdot10^{15}$	10^{16}	$5\cdot10^{16}$	10^{17}	$5\cdot10^{17}$	10^{18}
Γ	1.91	1.77	4.76	5.54	24.50	33.67	38.12	79.55	121.40	327.31	460.20
$\gamma\Gamma$	1.64	1.45	5.17	6.20	164.03	$2.39\cdot10^{4}$	$3.5\cdot10^{7}$	$1.69\cdot10^{7}$	$4.03\cdot10^{6}$	$4.19\cdot10^{6}$	$6.21\cdot10^{6}$
	T = 15K										
Nd(cm^{-3})	$3\cdot10^{12}$	10^{14}	$5\cdot10^{14}$	10^{15}	$5\cdot10^{15}$	$7\cdot10^{15}$	10^{16}	$5\cdot10^{16}$	10^{17}	$5\cdot10^{7}$	10^{18}
Γ	1.39	1.78	4.24	5.68	23.84	30.95	37.39	78.17	118.02	323.10	471.30
$\gamma\Gamma$	1.11	1.47	4.48	6.68	157.00	929.97	$6.40\cdot10^{6}$	10^{7}	$1.25\cdot10^{7}$	$1.32\cdot10^{7}$	$4.31\cdot10^{7}$
	T = 17K										
Nd(cm^{-3})	$3\cdot10^{12}$	10^{14}	$5\cdot10^{14}$	10^{15}	$5\cdot10^{15}$	$7\cdot10^{15}$	10^{16}	$5\cdot10^{16}$	10^{17}	$5\cdot10^{17}$	10^{18}
Γ	1.65	1.89	3.80	5.90	24.27	34.00	38.10	75.77	117.64	326.65	464.11
$\gamma\Gamma$	1.35	1.57	3.87	7.23	211.38	$6.74\cdot10^{3}$	$4.23\cdot10^{6}$	$2.64\cdot10^{6}$	$1.63\cdot10^{7}$	$5.58\cdot10^{6}$	$1.08\cdot10^{7}$
	T = 20K										
Nd(cm^{-3})	$3\cdot10^{12}$	10^{14}	$5\cdot10^{14}$	10^{15}	$5\cdot10^{15}$	$7\cdot10^{15}$	10^{16}	$5\cdot10^{16}$	10^{17}	$5\cdot10^{17}$	10^{18}
Γ	1.19	1.86	3.80	5.63	22.82	33.43	37.84	76.10	124.00	317.80	471.00
$\gamma\Gamma$	0.93	1.58	3.94	6.81	155.93	$1.34\cdot10^{3}$	$1.36\cdot10^{7}$	$2.60\cdot10^{7}$	$1.88\cdot10^{7}$	$3.33\cdot10^{7}$	$1.03\cdot10^{7}$
	T = 45K										
Nd(cm^{-3})	$3\cdot10^{12}$	10^{14}	$5\cdot10^{14}$	10^{15}	$5\cdot10^{15}$	$7\cdot10^{15}$	10^{16}	$5\cdot10^{16}$	10^{17}	$5\cdot10^{17}$	10^{18}
Γ	0.72	0.65	1.80	2.62	11.10	34.11	36.81	76.34	114.94	295.26	412.00
$\gamma\Gamma$	0.45	0.46	1.66	2.70	149.25	$3.60\cdot10^{7}$	$6.33\cdot10^{7}$	$5.74\cdot10^{7}$	$7.27\cdot10^{7}$	$1.18\cdot10^{7}$	$3.19\cdot10^{7}$
	T = 77K										
Nd(cm^{-3})	$3\cdot10^{12}$	10^{14}	$5\cdot10^{14}$	10^{15}	$5\cdot10^{15}$	$7\cdot10^{15}$	10^{16}	$5\cdot10^{16}$	10^{17}	$5\cdot10^{17}$	10^{18}
Γ	0.73	0.78	2.23	3.77	19.64	24.50	37.35	73.90	110.87	288.76	393.00
$\gamma\Gamma$	0.58	0.63	2.59	5.65	284.62	893.43	$3.20\cdot10^{7}$	$1.13\cdot10^{8}$	$1.08\cdot10^{8}$	$3.75\cdot10^{7}$	$1.14\cdot10^{7}$

phonon, are comparable. As the energy of the carriers increases, i.e., at higher temperatures and electric fields, equivalent intervalley phonon scattering predominates, and the conditions under which our model is valid, namely, when a single scattering mechanism dominates the scattering rate, are more closely approached. This leads to a better agreement of our predicted characteristics with the experimental ones. For samples of practical doping densities, we would expect our predicted results to closely agree with experiment. Additional results of this approach are shown in Figs. 3 and 4. Fig. 3 displays the electron drift velocity at a temperature of 10 K with various doping concentrations as a parameter. Fig. 4 shows the electron drift velocity as a function of electric field at a doping concentration of 10^{15} cm^{-3} with various temperatures as a parameter.

ACKNOWLEDGMENT

The authors thank Prof. M. S. Lundstrom and M. Klausmeier-Brown for most graciously providing their III-V compound Monte Carlo simulator, DEMON [12], which was adapted to perform the silicon high-field calculations needed in this work. Prof. M. S. Lundstrom, and Dr. F. L. Augustine from Hughes Microelectronics

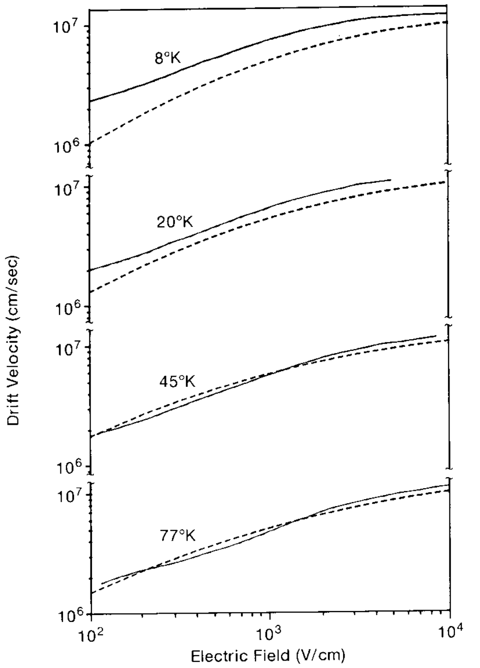

Fig. 2. Electron drift velocity as function of electric field at the indicated temperatures. Continuous and dashed lines refer to experimental and calculated values, respectively. The doping density is $NA = ND = 5 \times 10^{12}$ cm^{-3}, after [4].

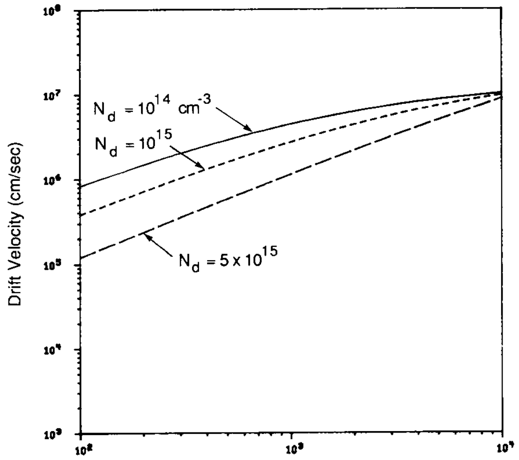

Fig. 3. Drift velocity as a function of electric field for various doping densities. $T = 10$ K.

Center, Carlsbad, CA, are especially thanked for reading the manuscript and providing useful comments. H. De Los Santos thanks Prof. B. Hoefflinger for his encouragement.

REFERENCES

[1] W. L. Engl, H. K. Dirks, and B. Meinerzhagen, "Device modeling," *Proc. IEEE*, pp. 10-33, Jan. 1983.

[2] D. M. Caughey and R. E. Thomas, "Carrier mobilities in silicon empirically related to doping and field," *Proc. IEEE*, pp. 2192-2193, Dec. 1967.

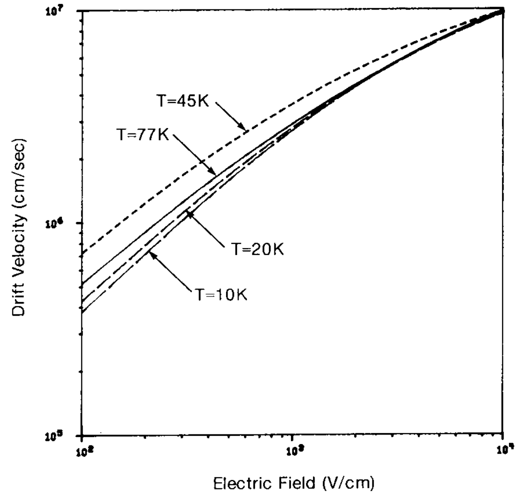

Fig. 4. Drift velocity as a function of electric field for various temperatures. $N_d = 10^{15}$ cm^{-3}.

[3] M. A. Omar and L. Reggiani, "Drift and diffusion of charge carriers in silicon and their empirical relation to the electric field," *Solid-State Electron.*, vol. 30, p. 683, 1987.

[4] C. Canali *et al.*, "Electron drift velocity in silicon," *Phys. Rev. B*, vol. 12, pp. 2265-2284, 1975.

[5] K. K. Thornber, "Relation of drift velocity to low-field mobility and high-field saturation velocity," *J. Appl. Phys.*, vol. 51, pp. 2127-2136, Apr. 1980.

[6] ——, "Applications of scaling to problems in high-field electronic transport," *J. Appl. Phys.*, vol. 52, pp. 279-290, Jan. 1981.

[7] C. Jacoboni and L. Reggiani, "The Monte Carlo method for the solution of charge transport in semiconductors with applications to covalent materials," *Rev. Mod. Phys.*, vol. 55, pp. 645-705, July 1983.

[8] G. L. Pearson and J. Bardeen, "Electrical properties of pure silicon and silicon alloys containing boron and phosphorus," *Phys. Rev.*, vol. 75, p. 865, 1949.

[9] E. M. Conwell and V. F. Weisskopf, "Theory of impurity scattering in semiconductors," *Phys. Rev.*, vol. 77, p. 388, 1950.

[10] E. M. Conwell, *High Field Transport in Semiconductors, Solid State Phys.*, suppl. 9. New York: Academic.

[11] W. Fawcett, A. D. Boardman, and S. Swain, "Monte Carlo determination of electron transport properties in gallium arsenide," *J. Phys. Chem. Solids*, vol. 31, pp. 1963-1990, 1970.

[12] M. E. Klausmeier-Brown, "Monte Carlo studies of electron transport in III-V semiconductor heterostructures," M.S.E.E. thesis, Purdue Univ., May 1986.

*

Hector J. De Los Santos was born in Santo Domingo, Dominican Republic, in 1957. He received the B.S. degree in electrical engineering from the University of Puerto Rico, Mayaguez Campus, in 1979, the M.S.E. degree in electronic circuits and systems from the University of California at Los Angeles in 1981, and the M.S.E.E. degree in solid-state devices from Purdue University, West Lafayette, IN, in 1985. He attended the University of California as a Hughes Fellow studying under Prof. G. C. Temes. He is currently working toward the Ph.D. degree in the School of Electrical Engineering, Purdue University.

At Purdue he has been a Patricia Roberts Harris Fellow and a Research Assistant since 1985. From January 1985 to August 1986, he was engaged in research in the area of BiCMOS circuits under the direction of Prof. B. Hoefflinger. Since August 1986, he has been doing research on the modeling of low-temperature transport mechanims in silicon, including hopping conduction, and on the computer modeling of impurity-band conduction IR detectors operating near liquid-He temperatures. While a participant in the Hughes' Engineering Rotation Program, he performed analysis and design for electronic circuitry of switching power supplies, worked on the implementation of a D/A converter test station including the design of a sampling voltage tracker, and designed a controller-motor interface. From 1981 to 1984, he was involved in the start-up of Intel Caribbean, Inc., Las Piedras, Puerto Rico, where he was responsible for the characterization of SRAM's and switched capacitor filters and codecs. His interests are in integrated circuits, in particular BiCMOS circuits and techniques, semiconductor physics, physics, and computer modeling of conventional and quantum transport processes and devices, and wave phenomena.

Mr. De Los Santos is a member of Tau Beta Pi and Eta Kappa Nu.

Jeffery L. Gray (S'81-M'82) received the B.S. degree in physics and mathematics in 1976 from the University of Wisconsin at River Falls and the M.S.E.E. degree in 1978 and the Ph.D. degree in electrical engineering in 1982 from Purdue University.

Currently an Assistant Professor of Electrical Engineering at Purdue University, his research interests include computer modeling of semiconductor devices, semiconductor device physics, extrinsic infrared detectors, and solar cells.